Experimental report

25/09/2019

Proposal: 5-54-185 **Council:** 10/2014

Title: A novel Skyrmion lattice topology in MnGe?

Research area: Physics

This proposal is a new proposal

Main proposer: Jonathan WHITE

Experimental team: Jonathan WHITE
Naoya KANAZAWA

Local contacts: Charles DEWHURST

Samples: MnGe

Instrument	Requested days	Allocated days	From	To
D11	6	0		
D22	6	0		
D33	6	5	27/04/2015	02/05/2015

Abstract:

Magnetic Skyrmions are well-established to exist in a small pocket of the magnetic phase diagrams of a range of chiral magnets, such as MnSi and FeGe. The Skyrmions typically form a 2D triangular lattice that can be described in terms of triple-q coupling of long wavelength single-q helically-modulated structures, and the resulting non-coplanar spin texture gives rise to novel emergent fields. MnGe is isostructural with the other Skyrmion hosts, yet displays a very different magnetic phase diagram with a remarkably large Skyrmion lattice (SkL) phase. Further, strong evidence indicates that the SkL topology in MnGe is not the conventional 2D triangular one, but instead is of novel 3D simple-cubic type. Until now however, experimental confirmation of this 3D cubic SkL has remained out of reach since only MnGe powder samples could be studied. Here we request 6 days on D33 to carry out a SANS study of newly available, and high quality single-crystalline MnGe thin films. The main goal is to confirm the existence of this new type of 3D SkL structure in MnGe, the topology of which is expected to support a new and novel lattice of emergent monopole and anti-monopole fields.

Experimental Report 5-54-185: A novel Skyrmion lattice topology in MnGe?

J.S. White[1], N. Kanazawa[2], C.D. Dewhurst[3], H.M. Rønnow[4], and Y. Tokura[2,5]

[1]*Laboratory for Neutron Scattering (LNS), Paul Scherrer Institute (PSI), CH-5232 Villigen, Switzerland*
[2]*Department of Applied Physics, University of Tokyo, Tokyo 113-8656, Japan*
[3]*Institut Laue-Langevin (ILL), 71 avenue des Martyrs, CS 20156, 38042 Grenoble cedex 9, France*
[4]*Laboratory for Quantum Magnetism (LQM), Institute of Physics, École Polytechnique Fédérale de Lausanne (EPFL), CH-1015 Lausanne, Switzerland*
[5]*RIKEN Center for Emergent Matter Science (CEMS), Wako 351-0198, Japan*

Introduction

Magnetic skyrmions are topological magnetic spin-vortex-like objects that can form in various non-centrosymmetric magnets [1]. In many skyrmion materials, such as the archetypal $B20$ chiral magnets MnSi and FeGe, skyrmions form string-like structures and form a 2D triangular skyrmion lattice (SkL) in a small phase pocket located just below the ordering temperature T_c and in a low magnetic field. Despite this widespread observation, different SkL topologies are expected in theory [2] - that could support exotic emergent phenomena. MnGe, also $B20$ material, is a known candidate for hosting a new type of SkL. In this material the topological Hall effect (THE), a hallmark experimental signature for topological spin texture formation is much larger in MnGe than for the other $B20$ compounds, and is observed over an unusually large portion of the magnetic phase diagram (see Fig. 1) [3]. Further, the reported observations indicate the topological phase can exist as a ground state, and over a much wider range of temperature and magnetic field compared with the small phase pocket in the other $B20$ compounds.

The magnetism underlying the unusual behaviour in MnGe was studied using SANS on a powder sample of MnGe [4]. In the earlier study the long-wavelength nature of helimagnetic order was confirmed, and suggestive evidence was obtained for the formation of a SkL in the region of the phase diagram relevant for the THE. Despite the evidence for a SkL state in MnGe however, direct confirmation of SkL formation, and its topology, remains elusive due to ambiguities arising from the powder nature of the available samples. The motivation for resolving these ambiguities comes from additional evidence from diffraction [3] that suggests the topological phase in MnGe should have either a 2D square or 3D simple-cubic topology, instead of the conventional 2D triangular one. Combining this result with theoretical modelling of the TH resistivity [4] leads to the emergence of a 3D simple-cubic topological 'hedgehog' lattice as the candidate topological magnetic structure in MnGe. If this new 3D SkL is confirmed, a new playground for emergent phenomena becomes accessible that is expected to include monopole and anti-monopole emergent fields [5].

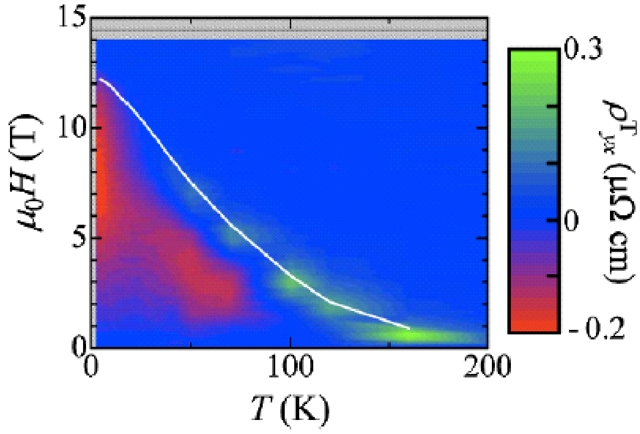

Figure 1: Magnetic phase diagram of MnGe. The white line indicates the field-polarised state. The red shading denotes where negative emergent fields are observed from THE data, and which denote the region where the possible cubic SkL is stabilised. From Ref. [3].

Experimental Method

Since bulk single crystal synthesis of MnGe is not possible at present, we took advantage of the recent breakthrough where epitaxially-grown and high quality, single-crystalline MnGe(111) thin films have been successfully grown on Si(111) substrates. For this growth configuration, two crystal domains nucleate with equal probability that are related by a 180° rotation around a common out-of-plane [111] axis. In this experiment we used SANS to explore the magnetic structures in a stack of 25 films that were each 160 nm thick, and 15 x 15 mm^2 cross-section. The stack of films were co-aligned and installed into a bespoke aluminium holder. The holder was then itself installed into a 2 T horizontal field cryomagnet mounted at D33. With the ability to rotate the magnet and sample stick independently, four experimental geometries were accessible; $\mu_0 H \| [111]$ ($\mu_0 H$ normal to the film plane) and $\mu_0 H \perp [111]$ ($\mu_0 H$ parallel to the film plane), with $\mu_0 H$ either parallel or perpendicular to $\mathbf{k}_i$. The majority of the SANS measurements were done in the geometry with $\mu_0 H \| [111] \perp \mathbf{k}_i$.

In our D33 SANS experiment we used neutrons with a wavelength of 3.35 Å (a short wavelength reached by tilting the velocity selector and inducing a 15 % FWHM in wavelength spread), an incoming collimation of 5.3 m and

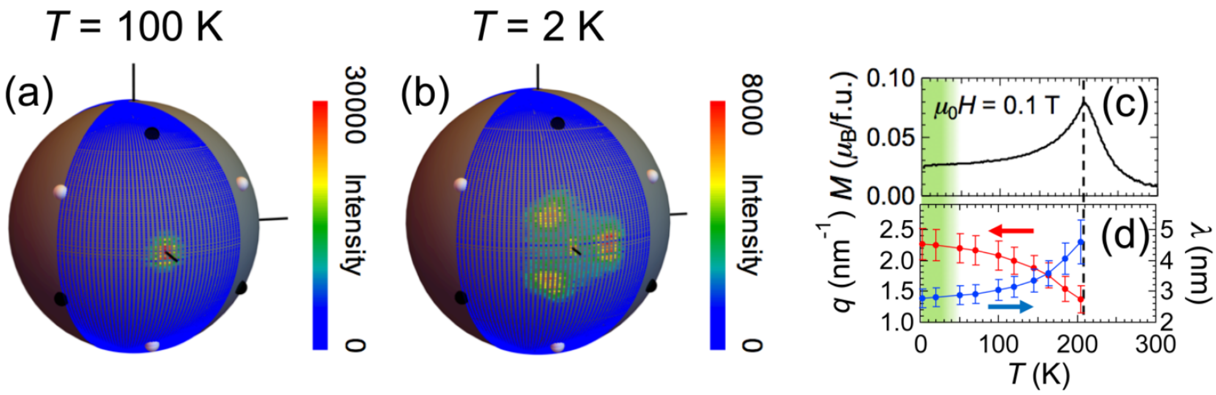

Figure 2: (a)(d) D33 data for 160 nm thick MnGe films: Scattering intensity maps on reciprocal space spheres at (a) high (T = 100 K) and (b) low (T = 2 K) temperatures. White and black dots represent the directions of the [100] crystalline axes of the two coexisting crystal domains. At 100 K the magnetic propagation vector is aligned with the out-of-plane (111) film axis. (c) The T-dependence of the magnetization 0.1 T, and (d) the magnitude of magnetic propagation vector q and magnetic period λ in zero field.

positioned the central 2D detector 2 m behind the sample. The SANS measurements were done in the usual way, by means of rocking scans where the magnet and sample were tilted or rotated together over an angular range that moved the SANS signal through the Ewald sphere at the detector. Measurements were done at selected magnetic fields and temperatures following various zero field cooling (ZFC) or field-cooling (FC) protocols. In $\mu_0 H$=0, rocking scans over an extended angular range were performed by rotating the sample stick only, and leaving the magnet in a fixed position.

Results

Despite a low magnetic scattering volume of the stack of 160 nm thick MnGe films, clear Bragg scattering was observed below the magnetic ordering temperature of approximately 202 K. We used D33 to map the distribution of propagation vectors describing the three-dimensional spin textures in reciprocal space by performing wide-angle rocking scans at various temperatures in zero field. We found that instead of the magnetic propagation vectors being aligned with the cubic axes of the film crystal lattice, at 100 K strong magnetic Bragg scattering is observed only at a single propagation vector aligned along (111) as shown in Fig. 2(a). This clearly shows uniaxial anisotropy, either in the form of shape or magnetocrystalline anisotropy, to play a decisive role on the chiral magnetism in these films. On cooling to lower temperatures we a transition in the magnetism is observed, which is characterised by a splitting of the single-q Bragg peak into at least three Bragg peaks, and so three wavevectors. As seen in Fig. 2(b), at the base temperature of 2 K the three magnetic wavevectors are tilted by about 10° from the (111) direction, and we interpret this observation in terms of a unique temperature-driven transition between single-q helical and a rhombohedrally distorted triple-q skyrmionic spin texture.

Figures 3(a)-(b) summarize the observed locations of magnetic Bragg spots at 2 K in stacks of 160 nm films studied here at D33, and stacks of 735 nm and 1800 nm MnGe films studied later in a similar manner at PSI. In all film thicknesses, the magnetic q-vectors are of identical magnitude, but the ground state tripe-q structures at low T each display different values of q-vector tilting angle θ from the out-of-plane (111) direction. Due to the different tilting angles of the q-vectors, the emergent magnetic field distributions in the magnetic unit cells are observed to vary as a function of the film thickness.

To describe the topological aspects of such a rhombohedrally distorted triple-q spin crystal more quantitatively, we start from the general expression

$$\mathbf{M}(\mathbf{r}) = \sum_{i=1,2,3} \mathbf{a}_i \cos(\mathbf{q}_i \cdot \mathbf{r}) + \mathbf{b}_i \sin(\mathbf{q}_i \cdot \mathbf{r}) \tag{1}$$

that describes a three-fold superposition of spin helices around a z-axis using $\mathbf{q}_1 = (\sin\theta, 0, \cos\theta)$, $\mathbf{a}_1 = (\cos\theta, 0, -\sin\theta)$, $\mathbf{b}_1 = (0, 1, 0)$, $\mathbf{q}_2 = (-\frac{1}{2}\sin\theta, \frac{\sqrt{3}}{2}\sin\theta, \cos\theta)$, $\mathbf{a}_2 = (-\frac{1}{2}\cos\theta, \frac{\sqrt{3}}{2}\cos\theta, -\sin\theta)$, $\mathbf{b}_2 = (-\frac{\sqrt{3}}{2}, -\frac{1}{2}, 0)$, $\mathbf{q}_3 = (-\frac{1}{2}\sin\theta, -\frac{\sqrt{3}}{2}\sin\theta, \cos\theta)$, $\mathbf{a}_3 = (-\frac{1}{2}\cos\theta, -\frac{\sqrt{3}}{2}\cos\theta, -\sin\theta)$, $\mathbf{b}_3 = (\frac{\sqrt{3}}{2}, -\frac{1}{2}, 0)$. The resulting magnetic texture is visualized in Figure 3(c), where magnetic moments with positive and negative z components (red and blue arrows) are seen to stack periodically along the z direction. Figure 3(d) shows the emergent magnetic field distribution calculated from the triple-q magnetic structure using $b_k = \frac{1}{2}\epsilon^{ijk}\mathbf{n}(\mathbf{r}) \cdot [\partial_i \mathbf{n}(\mathbf{r}) \times \partial_j \mathbf{n}(\mathbf{r})]$, where $\mathbf{n}(\mathbf{r}) = \mathbf{M}(\mathbf{r})/|\mathbf{M}(\mathbf{r})|$ [6]. Singularities in the emergent magnetic field distribution are found where the spin directions flip along the z direction. These points correspond to emergent magnetic monopoles (yellow points in Figure 3(d)) and antimonopoles (green points) which are connected by regions of positive and negative b_z (red and blue regions in Figure 3(d)). The yellow and green points respectively correspond to topological hedgehog [Figure 3(e)] and anti-hedgehog [Figure 3(f)] singularities, which are thus seen to form a periodic arrangement inside the film.

These results obtained at D33 on the stack of 160 nm thick MnGe films were further reconciled with magnetization and magnetotransport data, and later extensive magnetic field-dependent SANS data obtained at PSI. Overall we observe the formation of the three-dimensional spin crystal to coincide with the parameter space for nontrivial Hall signals, which further indicates the existence of a ground state three-dimensional topological magnetic order in the films. Later at PSI we performed further SANS measurements on the stacks of 735 nm, and 1800 nm thick MnGe films to determine the thickness-dependence of the rhombohedrally distorted triple-q spin crystal. The results of this study are reported in our publication [7].

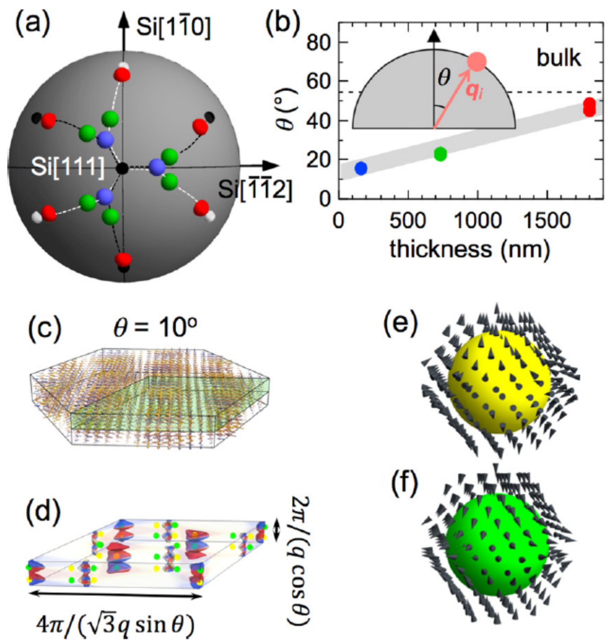

Figure 3: (a) View along the Si [111] axis for the reciprocal space sphere, showing the peak positions of the scattering intensity patterns at 2 K in zero field. Blue, green, and red spots denote the peaks observed from the 160 nm, 735 nm, and 1800 nm thick films, respectively. White and black dots represent the directions of the [100] crystalline axes of the two coexisting crystal domains. White and black dashed lines are guides for the eye, indicating the trajectories that scattering peak positions follow with changing the uniaxial magnetic anisotropy in the two domains (b) Thickness dependence of the angle θ between the film normal (MnGe [111] axis) and the q-vectors. The thick gray line is a guide for the eye. (c) Schematic illustrations of triple-q spin states with $\theta = 10°$. Red and blue arrows indicate spins with positive and negative z components, respectively. (d) Distributions of hedgehog singularities and the emergent magnetic field in the corresponding green box region of (c). Hedgehog [emergent monopole, (e)] and antihedgehog [emergent antimonopole, (f)] spin singularities appear where the spin directions flip.

Summary

To summarize our experiment, we used D33 to perform the first SANS measurements of the chiral helimagnetic and topological magnetic phases a stack of 160 nm thick MnGe films. Our data evidence the formation of a rhombohedrally-distorted triple-q spin crystal in the film, which is very much distinct to the cubic triple-q spin crystal expected for bulk MnGe. These results demonstrate more generally the pivotal role of magnetic anisotropy in the formation and control of versatile multi-q topological spin states in MnGe thin films. The artificial nanoengineering of the magnetic anisotropy is thus promising for expanding the range of topological spin textures that may generate novel functionalities based on emergent fields.

References

[1] N. Nagaosa and Y. Tokura, Nat. Nanotech. **8**, 899 (2013)

[2] B. Binz *et al.*, Phys. Rev. Lett. **96**, 207202 (2006)

[3] N. Kanazawa *et al.*, Phys. Rev. Lett. **106**, 156603 (2011)

[4] N. Kanazawa *et al.*, Phys. Rev. B **86**, 134425 (2012)

[5] H. Watanabe *et al.*, arXiv:1309.7047v1 (2013).

[6] N. Nagaosa and Y. Tokura, Phys. Scr. **T146**, 014020 (2012).

[7] N. Kanazawa, *et al.*, Phys. Rev. B **96**, 220414(R) (2017)